

# **MXene-Based Energy Harvesting Wearables**

**MATE 493 - Final 2019 Report**

Rebecca Schwartz, Natalia Noriega, Grayson Deysher

Mentors: Asia Sarycheva, Ariana Levitt

Advisor: Professor Yury Gogotsi

Drexel University

A.J. Drexel Nanomaterials Institute

Department of Materials Science and Engineering

Philadelphia, PA 19104

## **Contents**

Abstract.....	3
Introduction & Background.....	3
Materials Processing.....	4
1. $Ti_3AlC_2$ MAX phase synthesis.....	4
2. $Ti_3C_2$ MXene synthesis.....	4
Deliverables.....	5
1. MXene-based antenna.....	5
2. Free-standing films on PET.....	5
3. Spray coating onto PET.....	6
4. Screen printing and painting on fabric.....	6
5. Knitted MXene-coated yarns.....	7
6. MXene-based dielectric capacitor.....	8
7. Yarn-Coating Device.....	8
Characterization and Testing Plan.....	14
1. MAX phase purity.....	14
2. MXene purity.....	14
3. MXene particle size.....	14
4. MXene electrical conductivity.....	14
5. MXene-based antenna performance.....	14
6. MXene-based dielectric capacitor performance.....	14
Results and Discussion.....	15
1. MAX phase purity.....	15
2. MXene purity.....	15
3. MXene electrical conductivity.....	15
4. MXene-based antenna performance.....	17
5. MXene-based dielectric capacitor performance.....	19
Rectifying circuit.....	22
Budget.....	25
Environmental, ethical, and safety considerations.....	25
Conclusion.....	26
Future Work.....	26
References/Appendix.....	27

## **Abstract**

First discovered at Drexel University in 2011[1], MXenes are a new family of two-dimensional (2D) materials. These 2D carbides and nitrides have been shown to be useful for numerous applications including energy storage devices and wearable devices [reference for energy storage [2]. Here, in this project, we are taking the development of wearable devices further by enabling energy harvesting on-the-go using MXene-based components working in sequence. While many MXene-based devices and components have been developed, these components have yet to be incorporated into one complete system. To demonstrate the significance of this step in MXene research, a portable energy harvesting wearable system was developed that could allow for a portable energy source for the wearer. Portable energy provides people with the ability to do more while on the go. Batteries and supercapacitors currently have significant limitations such as weight, low cycles to failure, and the ability to only store limited amounts of energy which results in a need for frequent recharging or replacement. The MXene component system presented here alleviates several issues inherent with current energy sources. There were energy harvesting devices reported before [reference of MXene TENG, with Kathleen]. The system in this project is a rectifying antenna which was designed to harvest energy from ambient GHz-frequency electromagnetic (EM) signals [3-4]. A rectenna is a circuit that converts ambient EM signals to usable direct current (DC) that is able to be stored in a capacitor. MXene-coated yarns were produced as a way of creating components for the rectenna that can easily be knitted into a wearable device. The rectenna components required include a knitted MXene-based antenna to receive EM signals and a MXene-based dielectric capacitor to store the harvested energy. While there is still a great need for further optimization, the work presented here provides a foundation for other entire MXene-based systems to be created.

## **Introduction & Background**

MXene based devices such as supercapacitors [5], sensors [6], antennas [7], and circuits painted with MXene ink [8] have been demonstrated as their own isolated units. However, there is still a great need to build the connections between these components to create entire MXene-based systems that use more than one of the advantages that MXenes provide. While this is the underlying goal of this project, another exciting aspect is the potential for potable energy. In recent years, significant research has been done on the development of energy harvesting wearables to overcome the portability limitations imposed by the need for recharging devices containing batteries and/or supercapacitors. [9] Moreover, wearable devices have been gaining the interest of the scientific community due to the promising applications of self-powered devices used for the Internet of Things/Internet of Everything (IoT/IoE), a concept introduced by Kevin Ashton, co-founder of the Auto-ID Center at MIT in a presentation he made in 1999. [10] This concept refers to the replacement of human communication with devices and proposes a self-network which lies under the concept of energy harvesting wearables; no extra effort from the user is needed for a continuous self-powered device. [11]

Although a few energy harvesting devices have been created [12-13], researchers are still looking for alternative sources of renewable energy and more efficient ways of harvesting energy that can be integrated into wearable devices. Hoping to solve this challenge, here we present the results of an ongoing project consisting of incorporating a rectenna into fabric to harvest energy from Wi-Fi radiation. Several rectennas have been demonstrated with bulk commercial circuit components in several different circuit configurations which involve an antenna to receive EM signals. [4] The antenna is connected to a set of diodes that convert the received current from alternating to direct current. This circuit is then connected to a capacitor to store the harvested energy. One recent demonstration of a rectenna was published in *Nanotechnology*. Park et al. printed a rectenna on plastic foils and achieved more than 90% device yield

resulting in a wireless power transmission of 0.3 W. [4] Several research groups have demonstrated that the rectenna can work with bulk components but to our best knowledge it has not yet been integrated into textiles. [3-4]

While the textile industry is developing rapidly, the question of fabricating meters of conductive yarns still remains unsolved. Metal-coated yarns exhibit relatively low conductivity as well as lack of flexibility, therefore a new coating material is needed. [20] Our approach is to use a conductive 2D material – MXene. MXenes are 2D transition metal carbides and nitrides that were first discovered in 2011 at Drexel. [1] Moreover, there have been discoveries by the Drexel Nanomaterials Institute group which show the ability of  $Ti_3C_2$  MXene to be used for antennas [14] and planar supercapacitors. [15] Knitted MXene-based supercapacitors are currently being developed. [16] Combining current research developments as well as the previously mentioned components, a wearable garment which harvests EM energy with MXenes will be the final product of this proposed project.

There are several facets of this project which will be necessary to address the ongoing issue of portable energy harvesting devices. The steps necessary to build a wearable MXene based energy harvesting device include the following: design an efficient rectenna circuit, synthesize  $Ti_3AlC_2$  MAX phase and  $Ti_3C_2$  MXene, integrate a planar MXene-based antenna and capacitor into the circuit for testing, and develop highly conductive MXene-coated yarns for knitting antennas into a wearable.

*\*\*Note: For simplicity, we use “MXene” to refer to  $Ti_3C_2$  and “MAX” to refer to  $Ti_3AlC_2$ .\*\**

## **Materials Processing**

### *MAX phase synthesis*

The production of the MAX phase that will be used for this project will be large batches to minimize variations in composition. The MAX phase can be made in 150 g batches which is enough to satisfy the required amount of MXene for this project.  $Ti_3AlC_2$  MAX phase was synthesized by mixing a stoichiometric ratio of titanium carbide, aluminum, and titanium. The resulting mixture was ball-milled for 18 h with yttria-stabilized zirconia balls. The mixture was then heated in alumina crucibles in a tube furnace at a rate of 5 °C/min to 1500 °C and held at that temperature for 1 h before cooling down. [16] The produced block of MAX phase was then drilled using a carbide-tipped drill bit and then the resulting MAX powder was sieved to <75  $\mu$ m particles, which was then used to create two-dimensional  $Ti_3C_2$  MXene.

### *MXene synthesis*

The production of  $Ti_3C_2$  MXene has recently been scaled up to 100 g batches in a large reactor. This method will be used to minimize any variations in the properties of the resulting MXene. There are various synthesis procedures used for producing  $Ti_3C_2$ , however the current optimal procedure for achieving high electrical conductivity involves a mixture of hydrofluoric acid and hydrochloric acid. This acid mixture selectively removes the aluminum layer from the layered MAX phase structure. 2 g of the MAX phase powder was then stirred in a solution of hydrochloric acid, hydrofluoric acid, and deionized (DI) water at room temperature for 24 h. Afterwards, to wash out the acids, a series of centrifugation and decantation was repeated several times until pH>6. This resulted in a pH-neutral paste of multilayer MXene. 2 g of lithium chloride was then added to 100 mL of DI water and stirred until it was completely dissolved. The solution was then added to the multilayer MXene paste and shaken until hydrogen bubbles began to appear on the edges of the bottle indicating that the delamination process was initiated. The solution was stirred at room temperature for 18 h. The same process of centrifugation and decantation was repeated 6 times to

remove the lithium and chlorine ions. The resulting colloid of single flakes of MXene was stored in a refrigerator and sealed with parafilm to prevent oxidation.

## Deliverables

### *MXene-based Antenna*

From the wide variety of antenna types, the one chosen for this project was a dipole antenna, specifically a half-wave dipole, due to the simplistic design with highest gain (dB). It is given this name considering that the length of the antenna can be calculated by dividing the wavelength of the desired frequency of operation [22]. When receiving electromagnetic frequency, the antenna is most sensitive to EM fields whose polarization is parallel to the orientation of the element (Figure 1.a). In this case it is a balanced antenna because of its bilaterally symmetry, as shown in Figure 1.b.

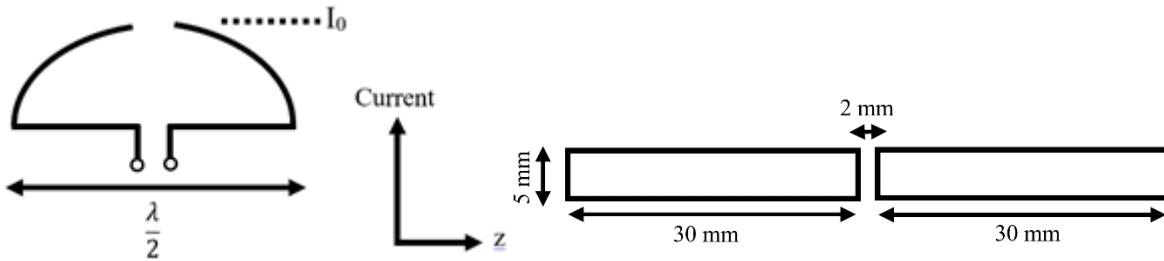


Figure 1. a) Electric current on a half-wave dipole antenna [18]; b) Dipole-Antenna Parameters of MXene Antenna to Collect Wi-Fi (2.4 GHz)

As previously mentioned, the electromagnetic signal that will be harvested is Wi-Fi signal, which is in the 2.4 – 5.9 GHz frequency range. Therefore, using equation 1, the wavelength of the desired frequency was calculated and divided to obtain the dipole antenna's length. [14] Having calculated the length of the antenna to be 60 mm, the following parameters shown in Figure 1.b were determined. The rectangles represent conductive material, which is the main requirement of an antenna. The distance between the conductive materials is negligible; the antenna is considered to be a single conductor connected via a coaxial SubMiniature version A (SMA) connector.

$$\lambda = c/f$$

Equation 1. Wavelength ( $\lambda$ ) determined by the speed of light ( $c$ ) over wave's frequency ( $f$ )

It was shown that MXene is possibly to be used as a conductor in an antenna [14] which can be processed through different techniques. The following techniques, filtering, spraying, screen printing, painting and yarn coating, were individually used to create MXene antennas with the objective to learn and choose the best signal harvesting device at the desired frequency.

### *Free-standing films on polyethylene terephthalate (PET) substrate*

Free-standing films were made by filtering 5 mL of a MXene colloid through a Celgard membrane (64 nm pores) in a vacuum assisted filtration system left overnight at room temperature. Then, following the determined parameters shown in Figure 1.b, two 30 mm by 5mm MXene films were cut and assembled

to a PET substrate using double-sided adhesive tape. An inner and outer part of a coaxial SMA connector were assembled to each of the two MXene conductive materials using a 1:1 ratio of Epoxy and hardener (Figure 2).

#### *Spray coating onto PET*

Antennas were also made by spraying colloidal MXene onto a plasma-cleaned 50  $\mu\text{m}$  thick PET sheet. The time of spraying was approximately 20 min until a uniform layer of MXene was visually perceived. Using the program Inkscape 0.91 the parameters (Figure 2) were designed. The antenna pattern was sculpted on the MXene spray-coated PET using an AxiDraw robotic arm (IJ Instruments Ltd.). Similarly, to the film technique, an inner and outer part of a connector were assembled to each of the two MXene conductive materials using a 1:1 ratio of Epoxy and a hardener.

It has been demonstrated that these two techniques, free-standing films and spray coating, can produce flexible MXene antennas due to MXene's 2-dimensional thickness and choice of flexible substrate. Quality of a transparent antenna can be maintained by varying the spray time and amount of colloidal MXene used. [14]



Figure 2. Transparent MXene Dipole Antennas of a) 62-nm-thick and b) 1.4- $\mu\text{m}$ -thick [10]

#### *Screen-printing and painting onto fabric*

A PET stencil was made by cutting the shape of the antenna's conductive rectangles using the parameters in figure 1b. As-synthesized MXene colloid was screen printed into fabric (100% cotton) using a paint roller and the PET stencil (Fig 3a.). Printed pattern was left to dry overnight and SMA connector was sawed to fabric for support and conductive epoxy was used to connect the SMA connector to MXene conductive material.

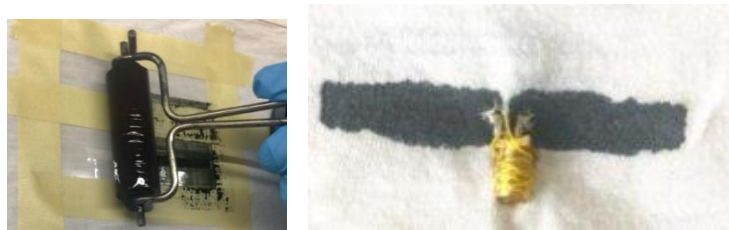


Figure 3. a) Screen printing technique on fabric using a PET stencil and a paint roller. b) Finalized antenna with SMA connector sawed to the fabric and connected to MXene conductive material using conductive epoxy

Additionally, 90 mL of as-synthesized MXene colloid were centrifugated for 20 min at 10,000 rpm and redispersed in 20 mL of DI water. The concentrated colloid was then probe sonicated for 20 min at 50% power, 8 s on, 2 s off, obtain smaller flake size for a better incorporation into the fabric. The concentrated MXene paste of smaller flakes was then painted onto fabric (Fig. 4.a). SMA connectors were then sawed with a cotton thread to hold them on place and using a 1:1 ratio of Epoxy and a hardener they were connected to the conductive MXene coated rectangles (Fig 4.b).

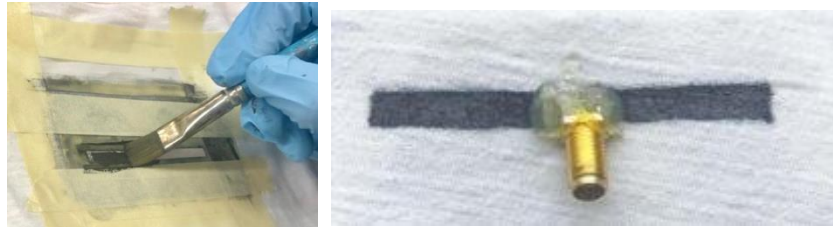


Figure 4. a) Painting technique on fabric using a PET stencil and a paint brush. b) Finalized antenna with SMA connector sawed to the fabric and connected to MXene conductive material using conductive epoxy and hot glue to improve insulate and improve connections

#### *Knitted MXene-coated yarns*

As-synthesized MXene was probe sonicated for 20 min at 50% power, 8 s on, 2 s off min to obtain smaller MXene flakes. With the aim of achieve the best performance of a knitted antenna nylon and cotton yarns were used. Two 0.9 m cotton yarns and two 0.9 m nylon yarns were coated by individually submerging the wrapped (to avoid tangling) yarns in a MXene-pool for 1 min, then taking the soaked wrapped yarns out of the pool for air-drying during 40 min, and finally unwrapping the yarns and letting them further dry for 10 min. This process was repeated about 12 times to achieve a low resistance which was measured using a multimeter.

Antennas were knitted using the MXene-coated yarn as the conductive material and uncoated yarns for non-conductive material surrounding the rectangles in Figure 1.b. The yarns were knitted at the Center for Functional Fabrics with the same parameters shown in Figure 1.b. SMA connectors were then sawed to the knitted structure (Fig 5) using cotton thread for support and connected using conductive epoxy.



Figure 5: Knitted antenna using MXene-coated nylon yarns as the conductive material and uncoated yarns for the non-conductive material. SMA connectors were sawed and connected to MXene-coated yarns using conductive epoxy.

### *MXene-based Dielectric Capacitor*

There are many publications which show that MXenes can be used as capacitor electrode materials. [3] Their high electrical conductivity and 2D geometry is what makes them suitable for capacitor applications. Although several types of capacitors (parallel plate, interdigitated, etc.) exist, a planar dielectric MXene-based capacitor will be used to simplify the circuit design. To fabricate a planar MXene-based capacitor, the colloid of  $Ti_3C_2$  MXene was sprayed using an air brush onto both sides of a plasma-cleaned PET substrate. After drying in a vacuum desiccator at room temperature, the planar capacitor could be cut to any size to achieve the desired capacitance. Typically, capacitance can be calculated with Equation 2 below, however MXene-based capacitors do not follow this equation. Therefore, this trend will be experimentally determined.

$$C = \frac{k\epsilon_0 A}{d}$$

Equation 2. Capacitance “C” of a parallel plate capacitor. “k” is the dielectric constant of the spacer material, “ $\epsilon_0$ ” is the permittivity of empty space, “A” is the cross-sectional area of the capacitor, and “d” is the spacing between the parallel plates.

MXene capacitors will be cut to various sizes to determine the effect that are has on capacitance. The amount of MXene sprayed onto each of the capacitors tested was the same to isolate area as the variable. In addition, the effect that resistance of each of the two MXene coated sides of the capacitor has on the capacitance was examined. This was done by spraying various amounts of MXene onto each side of the capacitors so that they would have different resistances. This way a potential relationship between resistance and capacitance could be explored.

### *Yarn-Coating Device:*

Mass production of MXene coated yarns is essential for knitting complete circuits. Without automation, coating several meters of yarns is a tedious, laborious process. With that, a yarn coating device was designed and built to produce 5+ meters of MXene coated yarns. The yarn would be fed through the machine, go through a MXene bath, and collect at a winder powered by a stepper motor. The number of coats is determined by the concentration of MXene colloid. [19]

The initial design requirements called for a 4-bath machine, with every roller mechanically powered. Each bath would be 0.3 minutes and each dry cycle would be 9 minutes. At the set linear velocity of 0.39 m/min (as consistent with a previously designed yarn coating device), the bearing pulleys which are 1 cm diameter, would rotate at 12.4 rpm. The winder would collect yarn at a rate of 1.13 rpm, with a diameter of 5.5 inches. That means that the motor shaft must rotate at 1.13 rpm to achieve the desired requirement of 11.7 cm of submersion per bath at any moment and 3.5 m of yarn drying per bath phase at any moment.

The original design's components included a 48” x 72” x ¾” wood board, base frame and wheels, an Arduino, a motor shield, two 12V worm gear DC motors, gears, tubing, wire, batteries and battery holder, bearings, shafts, shaft collars, screws, nuts, washers, and 3D parts designed in Creo software.

A 3-Dimensional drawing was made in Creo of the original yarn coating device. See Figure 6 below for a front and back view of the original design. Yarn (green) is routed through a series of rollers (in blue)

and on the way, go through a series of baths (curved yellow). A series of (60) gears work to turn the rollers in the appropriate direction to drive the yarn through the coating process. Worm-gear motors and an Arduino UNO were chosen in this design to drive the gears.

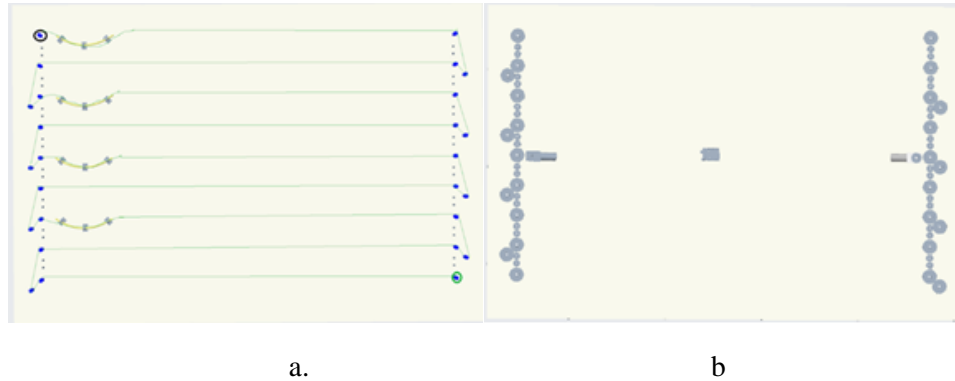


Figure 6. a) Front view of the first design iteration of the yarn coating device; b) Back view of the yarn coating device

After review, new design parameters were established to reduce complexity. Material selection for the device was also reviewed and redesigned to avoid damaging due to contact with liquid. The new design was greatly simplified, easy to use, and included more appropriate materials.

The new design, which ended up being built, has no gears, non-porous materials, and be small enough to work with on a tabletop such as a lab bench. Wood was determined to be a poor material for the yarn coater because of the possibility of the damage due to the wet environment. Instead of a wooden wheeled base, the new design's base and frame was made of plastic, fastened with machined L brackets. Instead of worm-gear motors and gears, a single stepper motor was used to power the winder. See Figure 7 below for a schematic of the Arduino Uno, stepper motor, motor driver, and potentiometer. Fritzing was used to draw the schematic. See Appendix 1 (A1) for the Arduino code. [20]

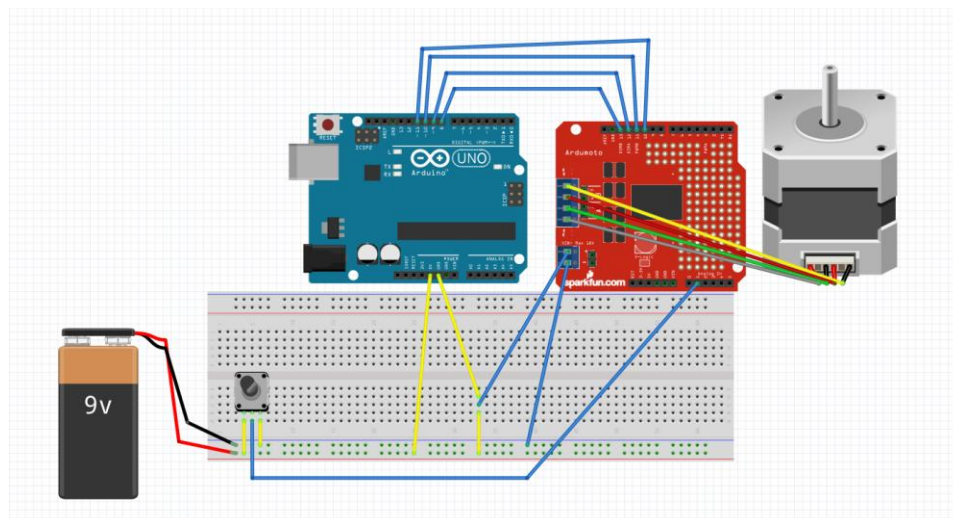


Figure 7. Schematic of Arduino Uno, stepper motor, motor driver, power source, and potentiometer

This set up allows for speed control by the user by simply turning the potentiometer. The lowest setting is no motion and the second lowest setting is 1 rpm.

Parts were carefully selected to ensure that they worked well as a system. The components of the yarn-coating device are shown below in Table 1. The build was completed at the Drexel Machine Shop. The vertical band saw was used to cut the plastic into sheets for the base and board. The horizontal bandsaw was used to cut 1 inch L brackets for structural stability. The drill press and milling machine were used to cut holes in the plastic and aluminum pieces for bolt placement. A lathe was used to sand roller shafts down to the right diameter for rollers. A power drill was used for bath holder placement.

Table 1: Yarn-Coating Device Components

Component Category	Component	Specifications	Quantity
Structural	Plastic	63" by 42"	1
	L brackets	1 inch wide; machined	20
	10-32 screws		20
Bath	silicone tubing	6mm id, 10 mm od, 5 m length	1
	3D printed tube holders	With inserts and bolts	3
Pulley	bearing pulley		5
	Long bolts	To hold rollers	4
Controller	Arduino UNO		1
	H-bridge		1
	potentiometer	10kohm	1
	set of wires		1
	breadboard		1
Motor	Stepper Motor	5mm diam shaft; 24 mm long; 20Ncm; 12V 350mA	1
	Aluminum plate to mount motor	8" by 4"	1
	bolts	to fasten motor to mount; A-2; 10 mm	4
	Plug-in power supply	Plugs in directly to Arduino; 9V, 12V	1
Winder	shaft	to attach to motor shaft; 1/4" diam; 3" length	1
	shaft coupler	5mm to 1/4" coupler	1
	metal brackets (4)	6.4" by 1.7" by 0.9"	1
	shaft collar	for 1/4" shaft diam	2
	female threaded standoff	where yarn collects; 1/4 od; 3" length; 6-32 threads	4
	bolts	for winder; 6-32 threads; 1/2"	4

The stepper motor was chosen through analysis of the torque required to rotate the winder. The torque can be found with Equation 3, 4, and 5 below. In equation 2, torque is defined as  $\tau$  (Nm),  $I$  is moment of inertia ( $\text{kg}\cdot\text{m}^2$ ),  $\alpha$  is angular acceleration ( $\text{rad}/\text{s}^2$ ). In equation 3,  $m$  is mass (kg),  $r$  is radius (m). In equation 4,  $\omega$  is angular velocity ( $\text{rad}/\text{s}$ ) and  $t$  is time (s).

$$\tau = I\alpha$$

Equation 3. Torque

$$I = \sum mr^2$$

Equation 4. Moment of Inertia

$$\alpha = \frac{d\omega}{dt}$$

Equation 5. Angular Acceleration

Angular acceleration was approximated to be about 0.1 rad/s<sup>2</sup>. Note that when the angular velocity is constant, the angular acceleration is zero theoretically. However in practice, angular acceleration was simply very close to zero, to take into consideration any minute changes in angular velocity.

The mass component of the moment of inertia is defined as a point mass. Therefore, the mass was approximately the sum of the masses of the female threaded standoff and bolt assemblies. The mass was 0.074 kg. The radius was 0.057 m. The moment of inertia was calculated to be 0.00024 kg m<sup>2</sup>.

It was assumed that there are no other outside forces. That is, the force due to friction was approximated to be zero since the friction of the bearing pulleys is negligible. The torque required to drive the system was determined to be 0.000024 Nm, which is 0.0024 N cm. The stepper motor selected was rated for 20 Ncm of torque, which is sufficient to power the winder even with a safety factor of more than 100.

Instead of powering every roller via a geared system, the new design only required power to a single shaft, which rotates the winder where yarn will be collected. Bearing pulleys guided the yarn along, thus acting as rollers. The rollers do not need to be powered because losses due to friction is negligible. Yarn was guided through a single bath in the same fashion as proposed in the original design. A curved tube acted as a bath of MXene colloid. Bath holders were 3D printed and were designed to hold the bath in place. A key feature of the bath holders is that the tube outer diameter can be as great as 11mm. An insert in the bath holders allows for different tubes to be swapped out. Tube inserts for 3mm, 5mm, 7mm, 9mm, and 11mm were designed. The inserts and tube holder have a tapped hole for a 10-32 bolt to keep the insert in place. As mentioned, the yarn was collected via a winder, which allows for additional drying of the yarn and greater surface area exposed to air than a simple roller would, thus increasing drying effect. The winder was powered by a stepper motor which will be controlled by an Arduino Uno. A potentiometer was used to control the speed of the winder. See Figure 7 below for a front offset and back offset view of the yarn coater.

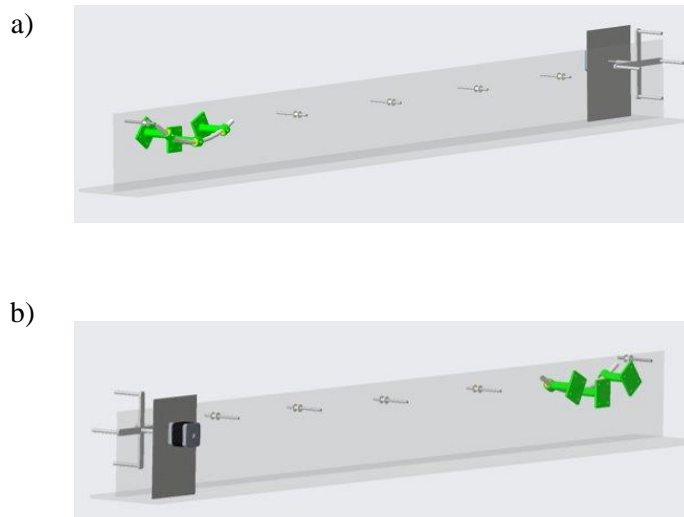


Figure 8. a) Front offset view of built yarn coating device. b) Back offset view of built yarn coating device.

Figure 9 below shows the actual yarn coater, highlighting key parts.

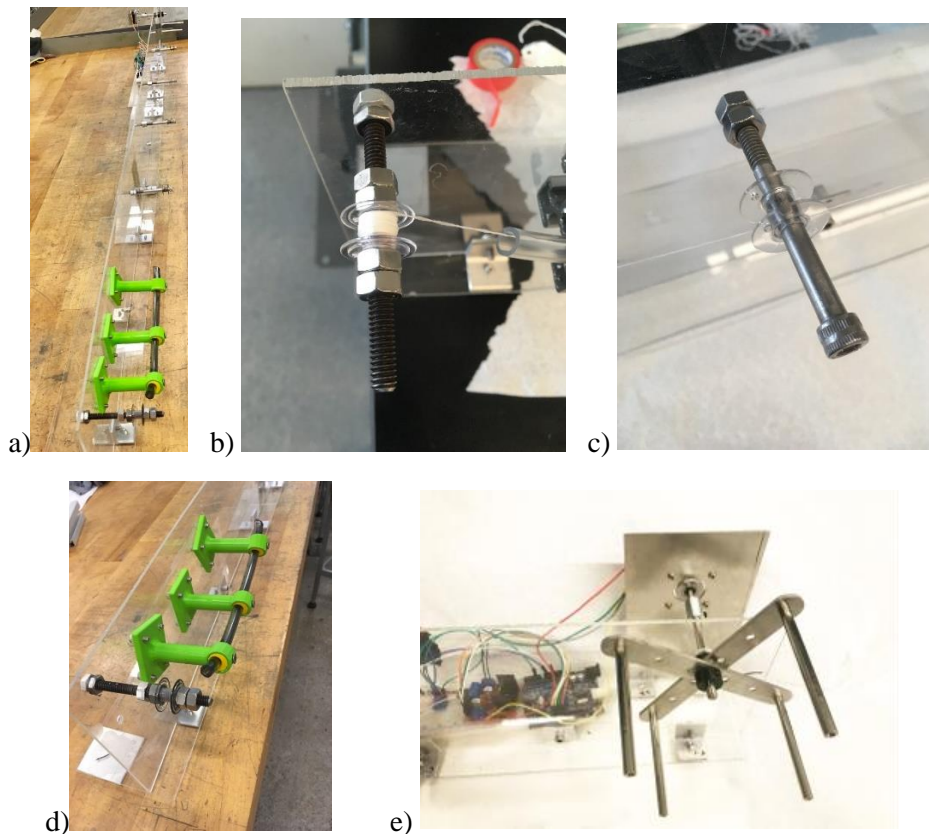


Figure 9. a) Yarn Coating Device. b) Initial roller where yarn begins its cycle. c) A typical roller and partially threaded bolt. d) A closer look at the bath (tube), bath holders and initial roller. e) Winder and Arduino set-up.

The yarn coater was used to coat 6.5 meters of nylon (see Figure 10 below). Thirty coats were applied. The resistance of the coated yarn was found to be about 100 ohm/cm. Through the coating process, an intricate procedure was followed to cut and rewind the yarn onto the original roller. The aim of the procedure was to get dry yarns back to the original roller without removing the yarn from the bath. To do this, 2 meters of sacrificial yarn were tied to either end of the nylon. Note that the yarn could not simply be reeled back to the original roller because then it would pass through the bath again, soaking the yarn and not giving it time enough to dry before the next coat.



Figure 10. Nylon with 30 coats of MXene colloid on yarn coater's winder.

Although the yarn coater made the yarn coating process simpler, it was determined that the design could be further optimized to minimize the need for human interface. A 3<sup>rd</sup> iteration of the yarn coater, as shown below in Figure 11, was designed so that the complicated resetting of the yarn could be eliminated. With two winders on either side of the bath, each winder would take turns rotating, allowing for ample drying time on either side of the bath. So, Winder A (lower winder) would rotate clockwise, pulling the yarn through the bath and giving enough time for it to dry as it collects. Once the yarn is all coated and collected, Winder B (upper winder) would rotate counter clockwise, pulling the yarn through the bath and allowing it to dry as it goes through the rollers and collects. The Arduino can be programmed to specify motor speed and timing for each winder. The only human interface would be setup, cleanup, and occasionally topping up the fluid bath. This was only a design and was not built because the previous version was sufficient for the amount of yarn needed for this project.

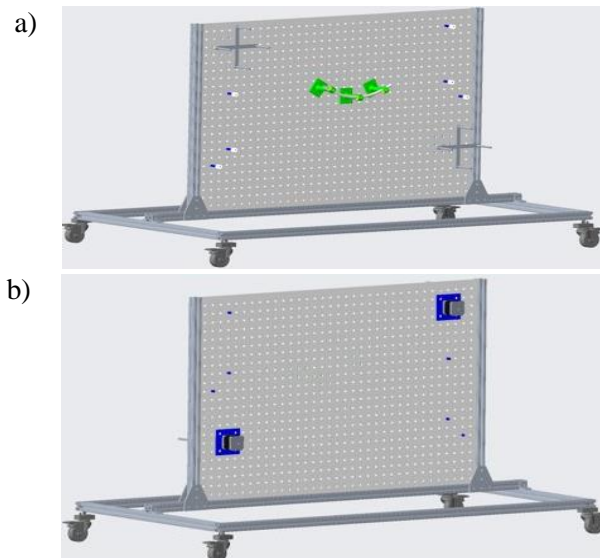


Figure 11. a) Front offset view of future yarn coating device; b) Back offset view of the future yarn coating device

## **Characterization and Testing Plan**

### *MAX Phase Purity:*

X-ray diffraction was performed on the sieved MAX phase powder on a Rigaku MiniFlex X-ray diffractometer. The sample powder was gently spread over the surface of the glass sample holder while avoiding pressing the powder.

### *MXene Purity:*

X-ray diffraction was performed on a filtered sample of single flake  $\text{Ti}_3\text{C}_2$ . The sample was placed on the glass slide and slightly deformed to the shape of the slide to increase its adhesion. This is important because during the measurement, the sample stage rotates which might cause the sample to fall off during measurement.

### *MXene Particle Size:*

Colloidal MXene was characterized by performing Dynamic Light Scattering (DLS) measurements of the hydrodynamic diameter of as synthesized MXene flakes. Using a plastic pipette, 1 drop (~30  $\mu\text{L}$ ) of MXene was diluted in 1 mL of DI water in a disposable polystyrene cuvette. The sample was equilibrated for 30 seconds before measurement and performed at 25 degrees Celsius.

### *MXene Electrical Conductivity:*

MXene conductivity was tested by measuring the resistivity of a MXene free-standing film using a 4-point probe. The MXene film was done by filtering the previously synthesized MXene colloid in a vacuum assisted filtration set up overnight at room temperature.

### *MXene-based Antenna Performance:*

The vector network analyzer (VNA) was used to measure the coefficient of reflection (S11 parameter) and the antenna working frequency. This was completed by connecting one port of the VNA to the MXene antenna in which the reference channel travels.

### *MXene-coated Yarns:*

The MXene coated yarns were characterized in a few ways. First is their resistance. This was measured with a multimeter at regular intervals at several regions of the 0.9 m long yarns. In addition, the mass loading of MXene on the yarns was measured by weighing the coated yarns and subtracting the initial weights of the yarns. This mass was then divided by the length of the yarns to obtain a mass loading with the units mg/cm. Scanning electron microscopy (SEM) was also used to ensure that the MXene was uniformly coated.

### *MXene-based Dielectric Capacitor Performance:*

The MXene-based capacitor does not obey Equation 2, so to determine how the capacitance changes with area, five different known sizes of the capacitor sheet were cut and tested (Figure 12). Each capacitor's capacitance was measured with a multimeter. The two leads of the multimeter were placed on opposite sides of the capacitors.

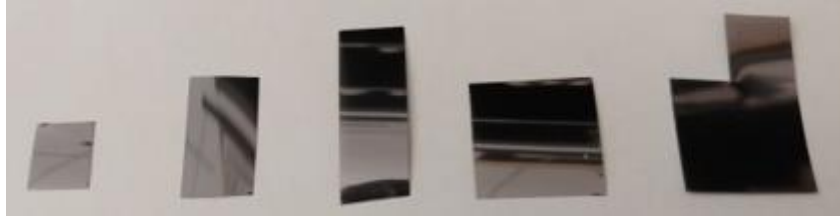


Figure 12. Sample MXene-based dielectric capacitors used for testing the dependence of capacitance on area. As shown the sizes from left to right are 1, 2, 3, 4, and 5 cm<sup>2</sup>.

To determine how the capacitance changes with resistance of each side of the capacitor, 10 sample capacitors were made. They are shown in Figure 13 below. The resistance values of each side of each capacitor were measured with a Jandel cylindrical four-point probe. Each side was measured at 10 points with the 4-point probe and averaged. The capacitance values were measured with a multimeter and allowed to settle on a value for 30 s before using the value.

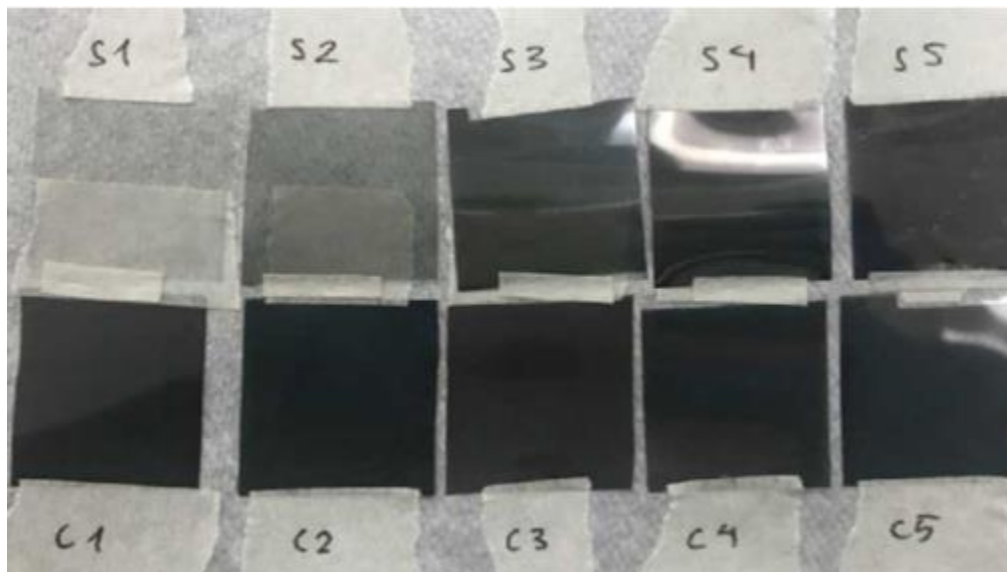


Figure 13. Sample MXene-based dielectric capacitors. S1-S5 denote the samples that have the same amount of MXene sprayed onto each side but vary from S1 to S2, etc. C1-C5 denote the samples that all have the same amount of MXene sprayed onto one side and then different amounts sprayed onto the other sides.

## **Results and Discussion**

### *MAX Phase Purity*

The X-ray diffraction (XRD) analysis performed on the MAX phase powder ensured its purity. The spectrum is shown below in Figure 14. After confirming that it contained only one MAX phase (Ti<sub>3</sub>AlC<sub>2</sub>), it was used to create two-dimensional Ti<sub>3</sub>C<sub>2</sub> MXene.

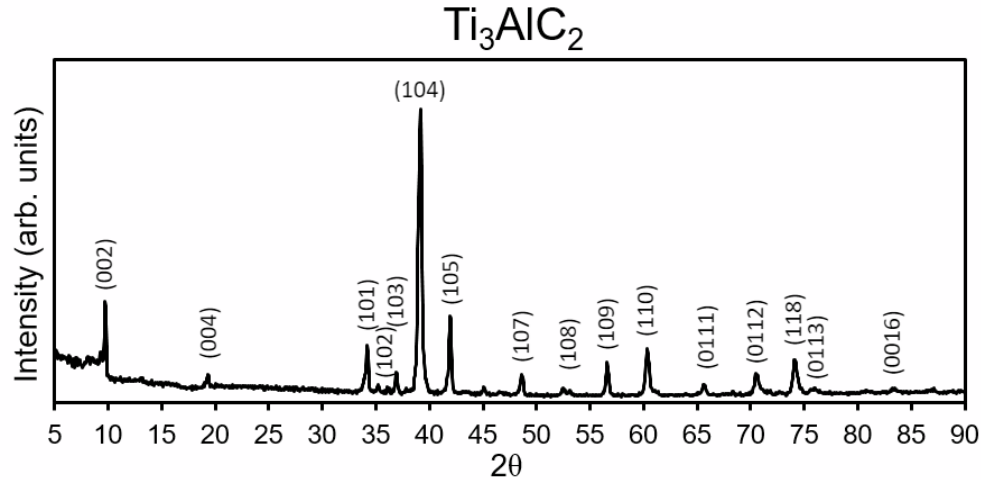


Figure 14. XRD spectrum of  $\text{Ti}_3\text{AlC}_2$  indicating the lack of other MAX phases which confirms the sample's suitability to be used to produce  $\text{Ti}_3\text{C}_2$  MXene.

#### *MXene Purity*

XRD analysis was also performed on a sample of MXene single flakes collected via vacuum-assisted filtration to ensure that the sample had been thoroughly etched and contained no multilayer or MAX phase impurities. The spectrum is shown below in Figure 15. After confirming its purity, the resulting colloid of single flakes of MXene was stored in a refrigerator and sealed with parafilm to prevent oxidation.

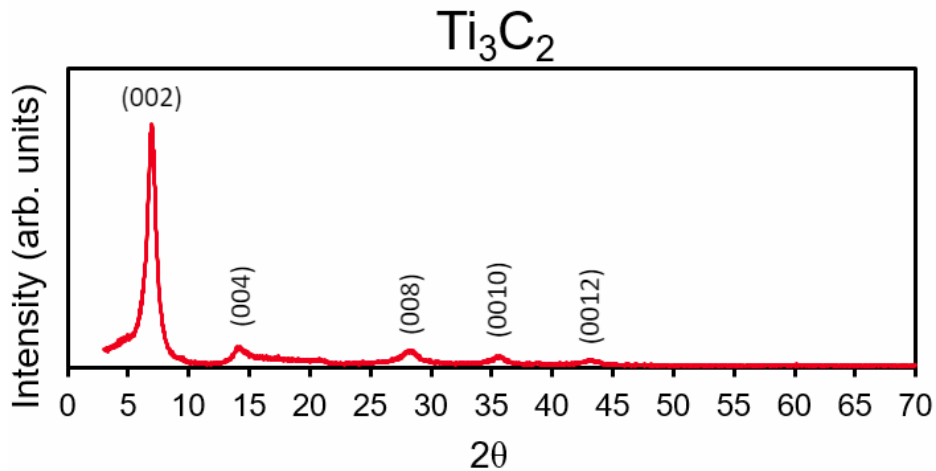


Figure 15. XRD spectrum of  $\text{Ti}_3\text{C}_2$  indicating the complete etching and delamination of the sample which concludes that it is suitable for MXene antennas and capacitors.

#### *MXene Electrical Conductivity*

Using the same free-standing MXene film collected via vacuum-assisted filtration, the conductivity was determined to be  $\sim 4,000$  S/cm. Due to previous limitations within the Nanomaterials Group, the MXene that was used for this study had a lower conductivity than is typical. Therefore, while the values from the

electrochemistry tests are not useable for developing this project, they do validate the fabrication method and once the synthesis issues are resolved, a high-performing device can easily be made for the product.

Furthermore, the conductivity is also dependent on the flake size, the higher MXene flake size, the higher conductive the material [21]. Using a Dynamic Light Scattering the hydrodynamic diameter resulted in ~850 nm. The size distribution vs. intensity graph is shown in Figure 16. The MXene flake size is also important for the adhesion to fibers, a higher flake size could result in an easy removal of MXene-coating from the fibers.

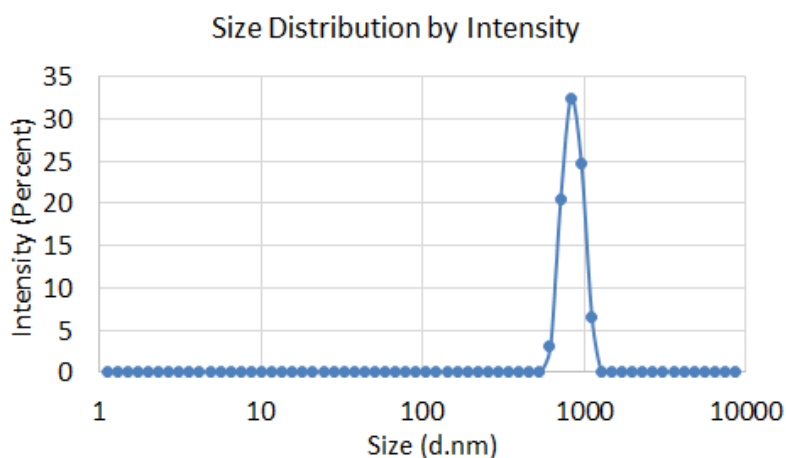


Figure 16. DLS results of the intensity distribution of  $\text{Ti}_3\text{C}_2$  MXene showing that the average flake size is 850 nm.

### *MXene-based Antenna Performance*

Even though the spray coating technique is ideal for making thin, transparent antennas, these properties are not necessary for the goals of the project. Furthermore, the robotic arm used to sculp the antenna pattern in the sprayed-MXene was deemed insufficient building the MXene antennas because it did not scrape completely the antenna pattern, failing to match the desired parameters. On the other hand, MXene antennas made with the film technique were successfully done and characterized.

The concentration of the as-synthesized MXene colloid which was used to screen print the antenna shown in Figure 3.b was calculated to be 3.5 mg/mL through vacuum-assisted filtration and weighing. It took 6 MXene-paint coats using the paint roller to achieve a resistance of 15 ohms which was measured after the last coat using a multimeter. Surprisingly, once the PET stencil was removed from the fabric after letting the MXene-printed rectangles dry overnight, the resistance had increased to 60 ohms even though it is expected to decrease resistance due to evaporation of water molecules. It was thought that removing the tape that was holding the stencil to the fabric had stretched the fabric and broken some MXene flakes connections. That is why the next technique did not include a stencil and instead, the concentrated MXene paste was used to paint the conductive rectangles (Fig. 4a) using a paint brush to improve precision (Fig 4b).

The painted antenna showed a lower resistance after only 3 coats of 9.8 ohms compared to the one made using the screen-printing technique which is explained by the higher concentration of MXene flakes. However, after the SMA connector was sawed, the resistance increased to 40.3 ohms. It is believed that the

pressure the needle placed against the fabric when sawing the SMA connector stretched the fabric to the point of breaking some connections between MXene flakes. Therefore, 2 more coats of MXene paint were needed to go back to a resistance of  $\sim 10$  ohms.

Even though connections between SMA connector and the conductive MXene rectangles were confirmed using the multimeter in all the antennas, VNA did not showed any predicted readings of any half-wave dipole antenna. Therefore, hot glue was used to insulate the connections to improve the performance of the antennas. Once connections were insulated, VNA measurements were taken to ensure that the working frequency of the antenna was that of Wi-Fi signal. In the x-axis of Figure 17, those antenna measurements that contain a downward peak (Film- and painted-antenna) imply that the antenna radiates best at that frequency. Meanwhile the y-axis indicates the reflection coefficient (S11 parameter) may be used to determine the electromagnetic wave reflected by an impedance of the film antenna.

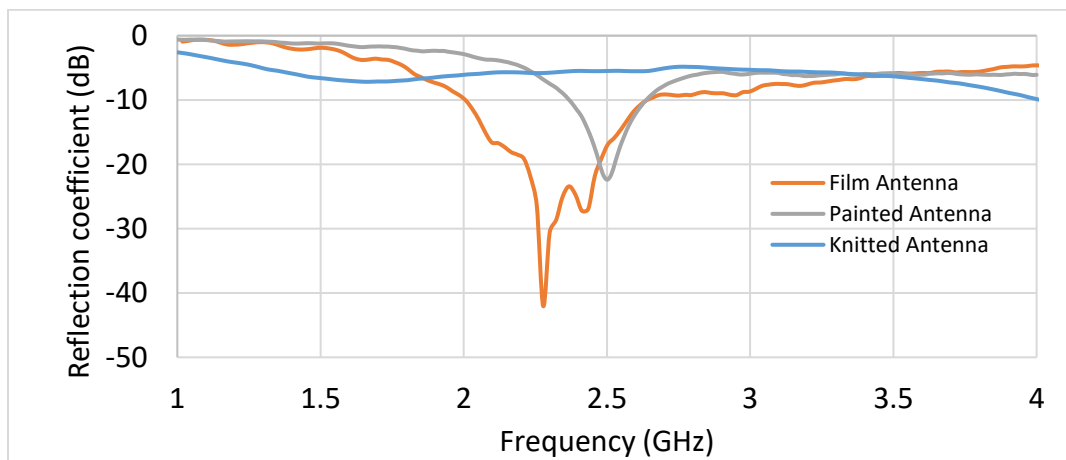


Figure 17. Vector network analyzer measurement of the reflection coefficient (dB) and the working frequency of a MXene-based antennas

The film antenna and the painted antenna had a reflection coefficient of -42 dB and -28 dB and best irradiation at a frequency of 2.38 GHz and 2.5 GHz, respectively. These results demonstrate the antennas' successful fabrication considering that it is well known in the antenna community measurements of any reflection coefficient value under -10 dB is characteristic of a working antenna. However, the change in frequency may be attributed to the change of length of the painted antenna due to the fabric substrate. Interestingly, the knitted antenna did not seem to work as results from the VNA did not showed any peak implying that the antenna did not radiated well at any frequency. The behavior may be attributed to the lack of connections between MXene-coated yarns due to the knitted structure as it was noticed that putting pressure against the antenna when it was being removed from the VNA resulted in an appearance of a downward peak. Therefore, to test the hypothesis that a knitted antenna may work if connections between coated yarns are improved, the following geometries (Figure 18) were done manually while testing.

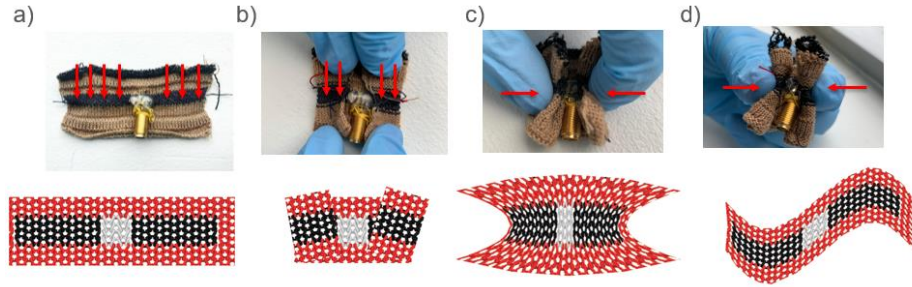


Figure 18. Antennas forced down using latex gloves on a) long-knit, b) half-fold, c) accordion fold and d) rolled structure during VNA testing.

In Figure 19, clear improvements from all the new geometrical antenna figures are shown. From all the folds, the half-fold antenna had the highest reflection coefficient of -25 dB, which is still indicative of a working antenna considering that the reflection coefficient is lower than -10 dB, and the rolled antenna of -45 dB. The changes in frequency may be explained from fact that by forming manually the different structures, there might be stretching of the knitted structure shifting to a lower frequency. Also, by rolling the antenna, connections may be improved significantly to the point of creating a thicker conductor of shorter length shifting to a higher frequency.

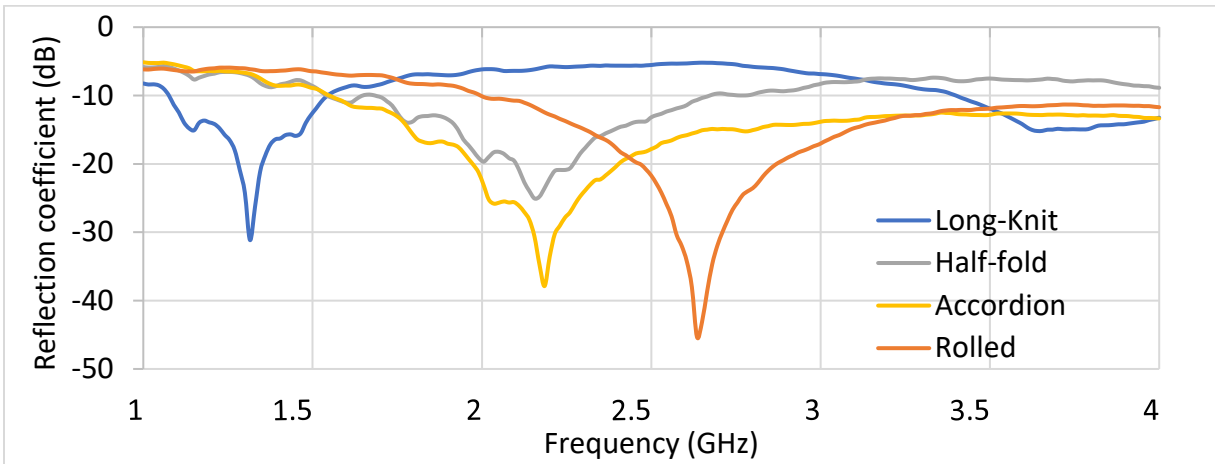


Figure 19. Vector network analyzer measurement of the reflection coefficient (dB) and the working frequency of different folds of knitted MXene antennas.

### *MXene-based Dielectric Capacitor Performance*

The results from the capacitance dependence on area tests for the MXene-based dielectric capacitor is shown below in Figure 20. The relationship has been determined to be linear which agrees with Equation 2 though the magnitude of the capacitance is vastly different, hence the need for a relationship for MXene specifically.

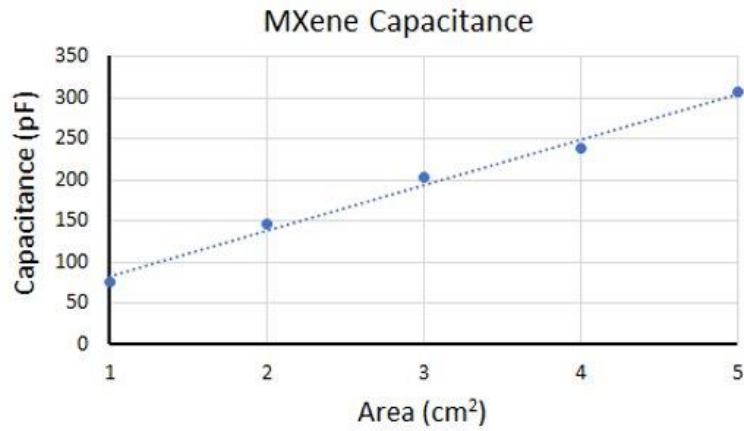


Figure 20. The linear dependence of capacitance on the area of the planar MXene-based dielectric capacitor.

Figure 21 below shows the resistance values of each side of each capacitor. They are in order of increasing amounts of sprayed MXene. As expected, as the amount of sprayed MXene increased, the resistance decreased. This is due to more  $Ti_3C_2$  flakes overlapping and creating more robust channels for electrons to flow.

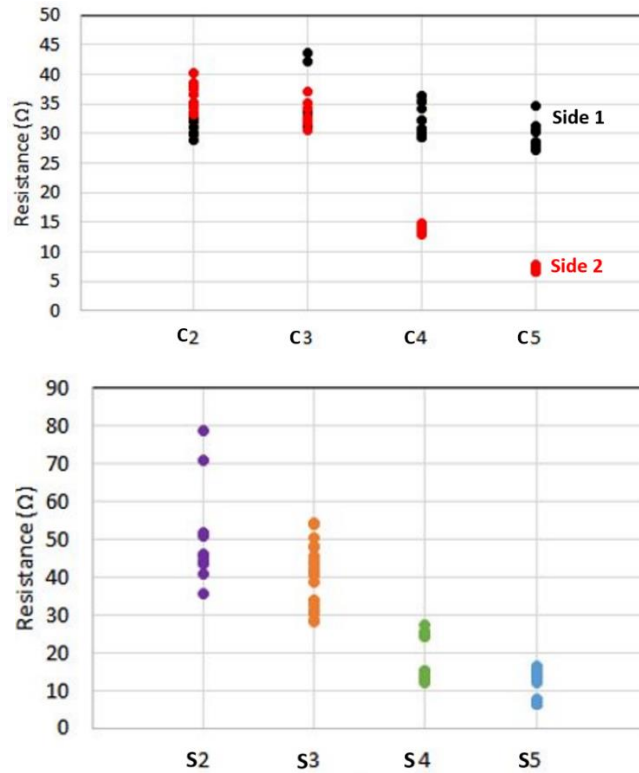


Figure 21. Resistance values of each of the capacitors. Top – Capacitors with the same amount of MXene sprayed onto their “Side 1” and then various amounts onto their “Side 2”. Bottom – Capacitors with the same amount of MXene sprayed onto both sides.

While measuring the capacitors used for the developing the relationship between area and capacitance was done by holding each of the two leads of the multimeter on opposite sides of the capacitor, that technique didn't work well for measuring these capacitors. The measured values were inconsistent. Some were even fluctuating between several orders of magnitude. To address this, copper tape was cut and pressed onto each of the two sides of the capacitors to form leads. This significantly improved the readings however there was still a large amount of fluctuation. Silver paint was then used to paint over the interface between the copper tape and the MXene coated capacitor to create an even better connection (Figure 22). This allowed for much more consistent values however there was still some drift by about 1-2 pF to higher capacitance values.



Figure 22. MXene capacitors with copper leads attached.

Since the measurements were done in the pF range, it seemed that even the humidity in the lab was slowly adsorbing onto the capacitors and screwing the results. To avoid this, the capacitors were placed in an argon glove box and any residual moisture was removed overnight. Afterwards, the measurements were extremely consistent and out of 10 measurements, varied by  $\sim 0.4$  pF. To account for any capacitance added by the copper tape and silver paint, a black capacitor was made with bare PET. The capacitance of this capacitor was measured and subtracted from the measured values of the MXene capacitors. Unfortunately, some of the capacitors were unable to be measured by the multimeter potentially due to short circuits created from the fabrication of the capacitor samples. The results from those measured are shown below in Figure 23. From this set of points a trend could not be determined as the capacitance values did not consistently increase or decrease though the capacitor with the highest resistance also had the lowest capacitance which would be expected.

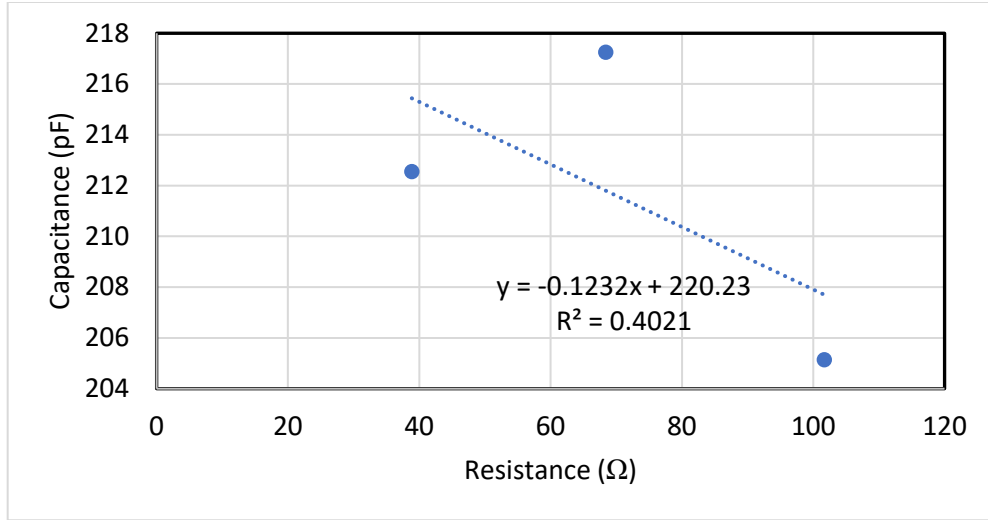


Figure 23. Capacitance as a function of total resistance of both sides of the MXene capacitors. No trend could be determined.

### Rectifying Circuit

To harvest and store power from an antenna, a rectifying circuit is necessary to convert alternating current to direct current. The typical rectifying circuit consists of a diode in series with a supercapacitor and a resistor in parallel with the supercapacitor (Fig. 24). Rectifying circuits were built using MXene-based components and bulk components for the purpose of testing efficiency. To target the efficiency of the circuit's components, the antenna was removed and replaced by a signal generator. The signal generator outputs power via alternating current expected to be transmitted by the antenna given a Wi-Fi signal. An oscilloscope was used to determine the output voltage waveforms of each circuit. This process would have helped to evaluate the performance of the rectifying circuit. Figure 24a shows a schematic of a half-wave rectifying circuit [17] and Figure 24b shows the built half-wave rectifying circuit [18]. This rectifying circuit was built with a copper tape substrate, a soldered coaxial cable, a high-frequency diode, a MXene supercapacitor, and a soldered resistor. The coaxial cable was soldered to the substrate to connect the circuit to a signal generator. However, without further characterization it was advised to use another non-conductive substrate in order to avoid unintentional electrical connections and short circuits.

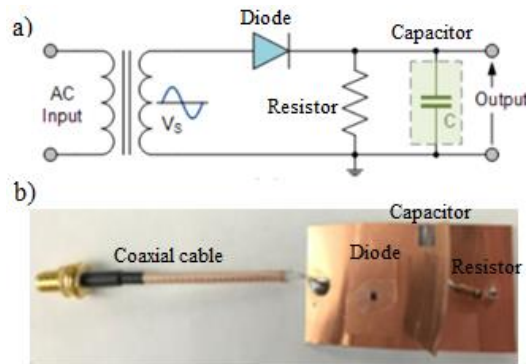


Figure 24. a) Schematic of a half-wave rectifying circuit design [17]; b) Circuit with copper tape, high-frequency diode, MXene supercapacitor, resistor and coaxial cable [18]

The next substrate of choice was a Printing Circuit Board (PCB), an epoxy glass fiber composite. PCBs are commonly used substrates for developing circuits due to their low dielectric loss. Two different circuits were fabricated; one made of only a PIN diode (Figure 25 a and b) and the other one with a PIN diode and MXene capacitor connect with copper tape (Figure 25 c and d). Electrical components were solder to the PCB using conductive epoxy, as cold solder, for the supercapacitor containing PET, and hot solder for the coaxial SMA connectors and the PIN diode. Two coaxial SMA connectors were attached to each circuit in order to easily input signal from a signal generator and read the converted DC using an oscilloscope. They were attached by soldering their inner part to the side of the substrate containing the electrical components and the outer part to copper tape in the opposite side of the substrate from where the electrical components were attached. The coaxial SMA connectors also served as grounding for each circuit.

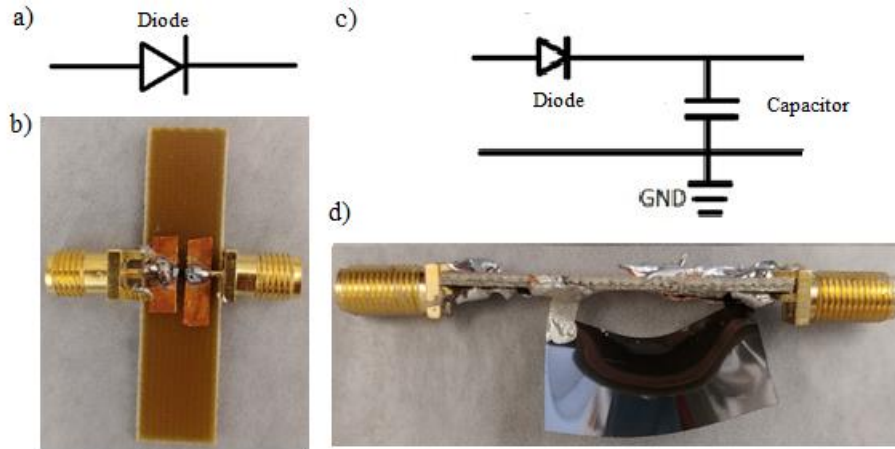


Figure 25. a-b) Circuit schematic and circuit in PCB composed of the two coaxial SMA connectors and a high-frequency diode; c-d) Circuit Schematic and circuit in PCB composed of two coaxial SMA connectors, a high-frequency diode and a MXene-based supercapacitor

The circuits were designed and measured starting with the simplest circuit and then the complete circuit including all components. The simplest circuit was the one composed of only the diode (Figure 25a), therefore an alternating signal will be inputted to the circuit with a signal generator and the oscilloscope will read the direct current once the diode has converted it (Figure 26). It should be noted that preliminary results of the circuit testing using a multimeter indicate that the circuit is indeed working however these results are not shown or discussed because no quantitative data could be generated.

A PIN diode was used considering it works in a high-frequency range which is required due to the Wi-Fi signal frequency (2.4GHz) instead of a low-frequency diode. The PIN diode (Figure 26.b) ideally transforms the alternative current generated by the signal generator (Figure 26.a) to a half-wave direct current (Figure 26.c) minus 250mW due to the power consumed by the PIN diode to transform the AC into DC.

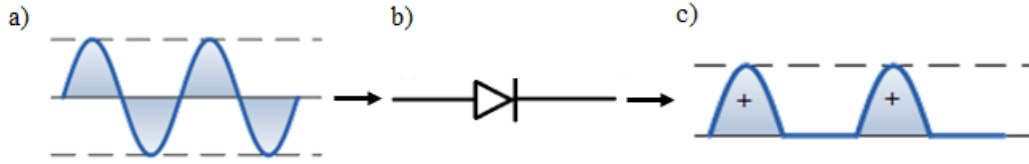


Figure 26. a) The input sine wave signal from the signal generator gets converted by (b) the high frequency diode to (c) a half-wave signal

Ideally, a 4-diode circuit shown in Figure 27 would be used to obtain a full-wave output. However, due to the low power (1 W) that a Wi-Fi router can generate, based on FCC rules and regulations, transforming the AC to DC with the 4-diode circuit would itself consume all of the power and not generate an output signal.

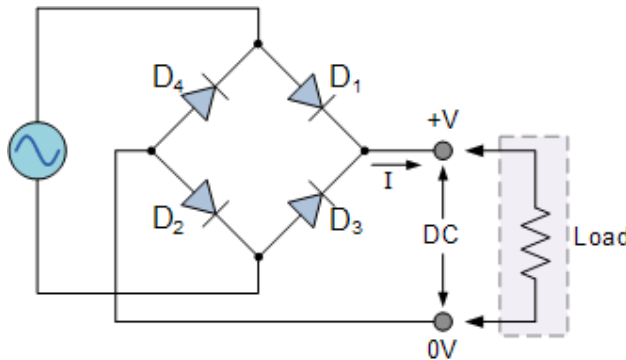


Figure 27. Schematic of a full wave rectifier using 4 diodes

Additionally, due to impedance matching it is well known that even a half-wave dipole antenna which has the highest gain will not transfer the entire power to the system. Therefore, considering that the signal generator in the circuit testing is replacing the antenna, an online calculator, that uses the Friis equations (Equations 6 and 7), was used to determine the MXene-antenna's theoretical output based on the antennas parameters; transmitted power (1 Watt), transmitter gain (6dB), frequency (2.4 GHz), receiver gain (2.1dB) [14]. Using these parameters typical of the previously fabricated and characterized MXene antenna, the theoretical output of the MXene antenna resulted to be 0.7089 W which will be the value used in the signal generator. It was expected that the oscilloscope read a power ~0.450 W in the circuit containing only the PIN diode (Figure 24b) due to the loss of power consumed by the diode.

$$P_{rx} = P_{tx} G_{tx} G_{rx} \left( \frac{c}{4\pi D_r f_0} \right)^2$$

$$P_{rx} = P_{tx} G_{tx} G_{rx} \left( \frac{c}{4\pi D_r f_0} \right)^2$$

Equations 6. and 7. Friis equations used to calculate antenna output power

The circuit containing the PIN diode and the MXene-supercapacitor (Figure 25d), was similarly tested. Figure 28. shows the expected oscilloscope reading and power output is expected to be lower than the one with only the diode ( $\sim 0.450$  W) due to some power loss from the MXene-supercapacitor.

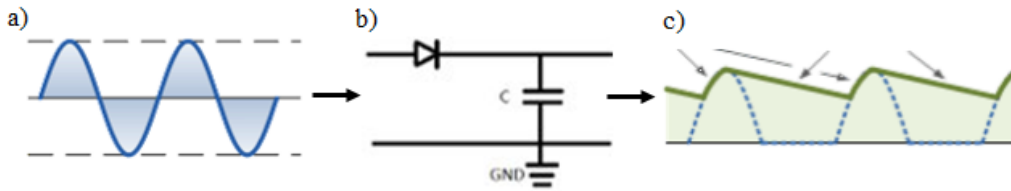


Figure 28. a) The input sine wave signal from the signal generator gets converted by (b) the high frequency diode and MXene-based dielectric supercapacitor to (c) a smoothed signal

Considering that successful results of the MXene-antenna and supercapacitor characterization were obtained and that the theoretical power transmitted by the MXene-antenna were used in the signal generator to input to the circuits, it is expected that integration of MXene-components to a circuit may be successfully achieved. Furthermore, the MXene components were designed to be integrated into wearables which facilitates the integration of the circuit to wearables as original proposed.

### **Budget**

The budget for this project is provided in detail in the Appendix A2, A3, and A4. Most of the projected cost is from indirect personnel and capital costs. The direct cost for the product itself is a very small percentage ( $\sim 1\%$ ) of the total budget. This is worth noting because if this product were to be mass produced for sale, the cost per unit would be low and much more affordable than the overall budget makes it seem.

### **Environmental, Ethical, and Safety Considerations**

The environmental, ethical, and safety concerns have not changed since last term and are still minimal. The main potential concerns for this project include the MXene itself, the effect that the antenna and circuit have on any implants in the wearer such as a pacemaker, the production of the garment, and the disposal of the garment. MXene has not been reported to be toxic to humans. The effect of the antenna and circuit on implants is unknown and would have to be tested if this product were to be mass produced and sold. The main concern with the mass production is the disposal of hydrofluoric acid-containing waste. There are no limitations on the fluorine content of sewer waste however the acids would have to be neutralized. There are no restrictions on the disposal of the garment however due to ethical concerns related to recyclability, an effort should be made to create a product with environmentally friendly materials.

### **Conclusion**

MXene components for Wi-fi energy harvesting were successfully fabricated and characterized. To the best of our knowledge, a knitted MXene-antenna was for the first time demonstrated. We proved that controlling knitted structures enables to decrease the reflection coefficient and change the frequency

of the antennas. Furthermore, MXene film capacitors were also fabricated to match any desired capacitance and an effort to develop a capacitance equation adequate to MXene capacitors was attempted. Alternatively, these components could still be useful immediately for other lower power applications such as sensors for hospital patients. Having successfully fabricated and characterized MXene-components are the first steps into developing energy harvesting wearables from MXene. Finally, the yarn coating device significantly reduced the effort, time and cost consumed by manually coating yarns with MXene.

### **Future Work**

Having demonstrated a working knitted antenna and presented a hypothesis on how the changes in the structure may influence the performance of the device, future work may include laminating the antenna with a polymer to (1) improve connections by insulating the knitted structure and (2) avoid MXene oxidation which would decrease conductivity. Furthermore, by analyzing the different folding structures and truly understanding the reasoning behind the change in frequencies, a formula may be developed considering that we have demonstrated that half-wave dipole knitted antennas do not followed the standard formula.

As for the yarn-coating device, the design for the future should be built for easier yarn coating. Additional development would also be required to incorporate the MXene-components into a working circuit. Based on the feasibility study performed, it is important to keep in mind the low voltage that could possibly be generated by the rectenna or any other circuit that harvest energy from Wi-Fi signal due to the low power FCC regulations. Further experiments should be performed into looking at alternative applications for these MXene-components.

## References

- [1] M. Naguib, M. Kurtoglu, V. Presser, J. Lu, J. Niu, M. Heon, L. Hultman, Y. Gogotsi and M.W. Barsoum, Two Dimensional Nanocrystals Produced by Exfoliation of  $Ti_3AlC_2$ , *Advanced Materials*, 2011, 23, 4248-4253.
- [2] Z. Zhou, W. Panatdasirisuk, T. S. Mathis, B. Anasori, C. Lu, X. Zhang, Z. Liao, Y. Gogotsi and S. Yang, Layer-by-layer assembly of MXene and carbon nanotubes on electrospun polymer films for flexible energy storage, *Nanoscale*, 2018, 10, 6005–6013.
- [3] S. Ahmed, Z. Zakaria, M.N. Husain, A. Alhegazi, Integrated rectifying circuit and antenna design with harmonic rejection for RF energy harvesting, *IEEE Xplore*, 2017, 11<sup>th</sup> EUCAP; 1940-1994.
- [4] H. Park, and H. Kang, Fully roll-to-roll gravure printed rectenna on plastic foils for wireless power transmission 13.56 MHz, *Nanotechnology*, 2012, 23, 3344006.
- [5] Wen, Y., Rufford, T.E., Chen, X., Li, N., Lyu, M., Dai, L. and Wang, L., 2017. Nitrogen-doped  $Ti_3C_2Tx$  MXene electrodes for high-performance supercapacitors. *Nano Energy*, 38, pp.368-376.
- [6] Kim, S.J., Koh, H.J., Ren, C.E., Kwon, O., Maleski, K., Cho, S.Y., Anasori, B., Kim, C.K., Choi, Y.K., Kim, J. and Gogotsi, Y., 2018. Metallic  $Ti_3C_2T_x$  MXene gas sensors with ultrahigh signal-to-noise ratio. *ACS nano*, 12(2), pp.986-993.
- [7] Sarycheva, A., Polemi, A., Liu, Y., Dandekar, K., Anasori, B. and Gogotsi, Y., 2018. 2D titanium carbide (MXene) for wireless communication. *Science advances*, 4(9), p.eaau0920.
- [8] Quain, E., Mathis, T.S., Kurra, N., Maleski, K., Van Aken, K.L., Alhabeb, M., Alshareef, H.N. and Gogotsi, Y., 2019. Direct Writing of Additive-Free MXene-in-Water Ink for Electronics and Energy Storage. *Advanced Materials Technologies*, 4(1), p.1800256.
- [9] S. Davis, Body Heat Can Be the Source of Power for Wearable Devices, *Technologies, Alternative Energy*, 2017. [Online]. Available: [www.powerelectronics.com](http://www.powerelectronics.com) [Accessed Mar. 10, 2019].
- [10] S. Madakam, R. Ramaswamy and S. Tripathi, Internet of Things (IoT): A Literature Review, *Journal of Computer and Communications*, 2015, 3, 164-172.
- [11] K. Shafique, B. Khawaja, M.D. Khurram, S.M Sibtain, Y. Siddiqui, M. Mustaqim, H.T. Chattha and X. Yang, Energy Harvesting Using a Low-Cost Rectenna for Internet of Things (IoT) Applications, *IEEE Access*, 2018, 6, 30932 – 30941.
- [12] Z.L. Wang and J. Song, Piezoelectric Nanogenerators Based on Zinc Oxide Nanowire Arrays, *Science*, 2006, 312, 242-246.
- [13] F. Fan, Z. Tian, and Z.L. Wang, Flexible Triboelectric Generator, *Nano Energy*, 2012, 1, 328-334.
- [14] A. Sarycheva, A. Polemi, Y. Liu, K. Dandekar, B. Anasori and Y. Gogotsi, [2D Titanium Carbide \(MXene\) for Wireless Communication](#), *Science Advances*, 2018, 4, eaau0920.
- [15] Q. Shan, X. Mu, M. Alhabeb, CE. Shuck, D. Pang and X. Zhao, Two-dimensional vanadium carbide ( $V_2C$ ) MXene as electrode for supercapacitors with aqueous electrolytes, *Electrochemistry Communications*, 2018, 96, 103-107.
- [16] L. Xinpo, and Y. Zhou, Pressureless sintering and properties of  $Ti_3AlC_2$ , *International journal of applied ceramic technology*, 2010, 7, 744-751.

[17] Power Diodes used as Half-wave Rectifiers, Basic Electronics Tutorials, 2019. [Online]. Available: [www.electronics-tutorials.ws](http://www.electronics-tutorials.ws) [Accessed: Mar. 18, 2019]

[18] M. Lukatskaya, O. Mashtalir, C.E. Ren, Y. Dall'Agnese, P. Rozier, P.L. Taberna, M. Naguib, P. Simon, M.W. Barsoum and Y. Gogotsi, Cation intercalation and high volumetric capacitance of two-dimensional titanium carbide. *Science*, 2013, 341, 1502-1505.

[19] J. A. Hodan, Yarn Coating Applicator, United States Patent: US005181401A, 1993.

[20] Coeleveld.com. (2019). *Arduino + Stepper (L298N) | coeleveld.com*. [online] Available at: <https://coeleveld.com/arduino-stepper-l298n/>

[21] K. Maleski, C. E. Ren, M.-Q. Zhao, B. Anasori and Y. Gogotsi, Size-Dependent Physical and Electrochemical Properties of Two-Dimensional MXene Flakes, *ACS Applied Materials and Interfaces*, 2018, 10, 24491–24498.

[22] P. J. Bevelacqua, The half-wave dipole antenna, 2018, [antenna-theory.com](http://www.antenna-theory.com/antennas/halfwave.php) [online]. Retrieve from <http://www.antenna-theory.com/antennas/halfwave.php>

## **Appendix:**

---

```
#include <Stepper.h>

const int stepsPerRevolution = 200; // change this to fit the number of steps per revolution
// for your motor

// initialize the stepper library on pins 8 through 11:
Stepper myStepper(stepsPerRevolution, 8, 9, 10, 11);

int stepCount = 0; // number of steps the motor has taken

void setup() {
  // nothing to do inside the setup
}

void loop() {
  // read the sensor value:
  int sensorReading = analogRead(A1);
  // map it to a range from 0 to 100:
  int motorSpeed = map(sensorReading, 0, 1023, 0, 50);
  // set the motor speed:
  if (motorSpeed > 0) {
    myStepper.setSpeed(motorSpeed);
    myStepper.step(stepsPerRevolution / 200);
  }
}
```

## Appendix A1. Arduino Code

Item	Cost
Circuit Components	\$150
Yarn	\$30
Yarn Coater	\$370
MXene	\$50
Other	\$200
Total	\$800

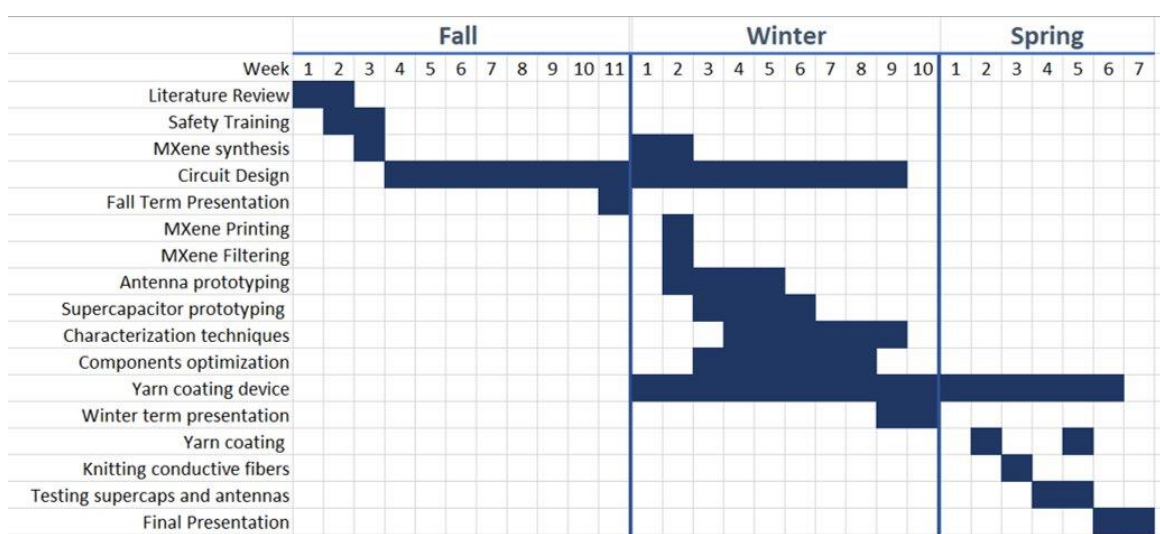
Appendix A2. Direct cost of the project components

Personnel	Hours	Hourly rate (\$/hr)	Cost
Advisor	20	50	\$1,000
Mentors	170	30	\$5,100
Seniors	850	20	\$17,000
Other	100	30	\$3,000
Total			\$26,100

Appendix A3. Indirect cost of the personnel

Capital	Hours	Hourly rate (\$/hr)	Cost
Lab & Equipment	700	50	\$35,000
Total			\$35,000

Appendix A4. Indirect capital cost



Appendix A5: GANTT Chart